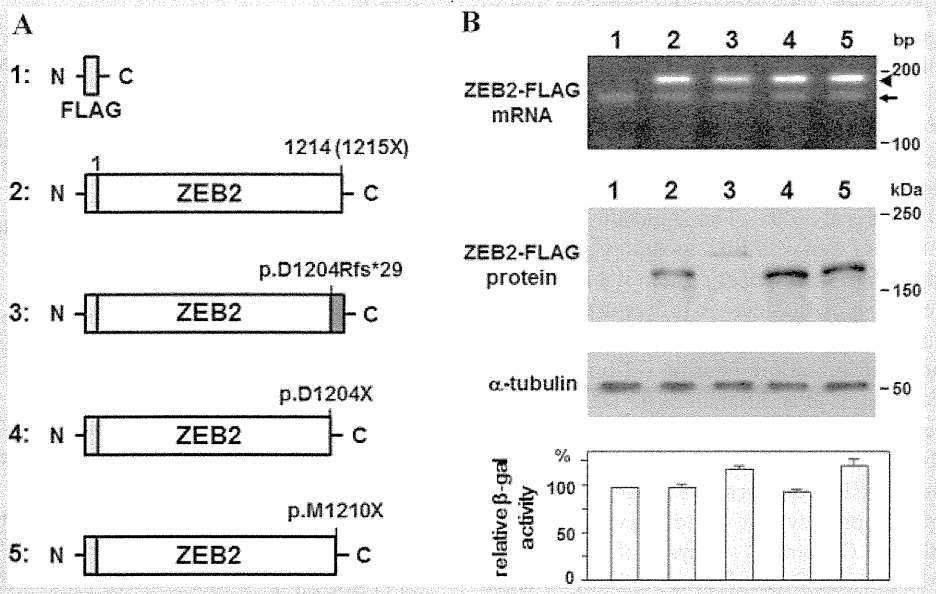

FIG. 2. Expression of wild-type and mutant ZEB2 proteins in HEK293 cells. A: A schematic illustration of FLAG-tagged ZEB2 mutants. B: First (topmost) panel. Multiplex PCR analysis of the FLAG tagged ZEB2 mRNA levels relative to ACTB in HEK293 cells transfected with each of the ZEB2-expressing vectors. Arrow and arrowhead indicated the PCR products of ACTB and FLAG tagged ZEB2, respectively. Second and third panels: Western blot analysis of HEK293 cells transfected with each of the ZEB2-expressing vectors using antibodies specific for FLAG and α-tubulin. Fourth panel: relative *E. coli* β-galactosidase (β-gal) activities in each transfected group of HEK293 cells. The vertical bars indicate the standard error of the mean for three experiments. Lane 1, pFLAG vector; lane 2, wild-type pFLAG-ZEB2; lane 3, pFLAG-ZEB2-D1204Rfs*29; lane 4, pFLAG-ZEB2-D1204X; lane 5, pFLAG-ZEB2-M1210X.

Japan recognize MWS based on the characteristic facial appearance and moderate or severe intellectual disability, similar to that seen in Down syndrome. There is no obvious genotype–phenotype correlation in the MWS patients except for large deletions (>10 Mb) at the 2q22-24 locus [Zweier et al., 2003; Ishihara et al., 2004]; yet we speculate that clinical features of MWS may become rather unclear when we include the deletion types harboring wide clinical symptoms. Thus, we have focused on the clinical features of MWS caused by nonsense and frameshift mutations in *ZEB2* in this study. We have identified 13 nonsense and 27 frameshift *ZEB2* mutations in 40 newly identified MWS patients. Thus, the overall number of nonsense and frameshift mutations of the so far identified Japanese MWS patients are 29 and 34, respectively, including those from previous studies [Yamada et al., 2001; Ishihara et al., 2004; Sasongko et al., 2007; Ohtsuka et al., 2008]. All the patients have the characteristic facial appearance, and moderate or severe intellectual disability. Compared to previous reports of the clinical summary of MWS including deletion cases [Dastot-Le Moal et al., 2007], the frequencies of patients showing seizures, abnormalities of corpus callosum, or congenital heart disease are quite similar; however, the frequencies of microcephaly (62% vs. 80%), Hirschsprung disease (38% vs. 54%), and urogenital/renal anomalies (30% vs. 52%) are lower than those previously reported (Table III) [Garavelli et al., 2009]. We observed that microcephaly is evident at a later age in some patients. For example: (1) S-090, occipitofrontal circumference (OFC): −1.0 standard deviation (SD) (at birth) and −2.5 SD (3 years old), (2) S-106, OFC: 0 SD (at birth) and −2 SD (9 years old) with failure to thrive. Thus, microcephaly may not be characteristic of the younger patients (~6 years old) in this study. Further case studies are necessary to investigate whether nonsense and frameshift mutations in *ZEB2* are responsible for the relatively lower number of Hirschsprung disease and urogenital/renal anomalies in this study. In addition, the urethral stones (S-062), spleen hypoplasia (S-112), chordee without hypospadias (S-120), duplicated renal pelvis (S-110 and P-1), and spinal bifida (K-02) identified in this study are rare in MWS. Further case studies are also necessary to establish whether these are symptoms associated with MWS. We found that two patients (S-101 and S-128) have self-injuries, in accordance with a recent study showing that MWS was associated with significant levels of behavioral and emotional problems [Evans et al., 2012].

In this study, using transient transfection, we demonstrated that the ZEB2-D1204Rfs*29 protein has a larger mass, but its protein level was remarkably decreased without a remarkable change in the mRNA level when compared to that of the wild-type ZEB2. Thus, MWS was caused by the ZEB2 protein instability in S-121. The D1204Rfs*29 mutation generates a new terminal codon. Consequently, the 11 C-terminal amino acid sequence (DHEEDNMEDGM) encoded by wild-type ZEB2 was replaced by a 28-amino acid sequence (RGRQYGRWHVNYCILSFHFFFPVVLLPA) by the frameshift mutation. Comparing the two C-terminal peptides, 6 (underlined) out of 11 amino acids were negatively charged

amino acids, while 15 (double underlined) out of 28 amino acids were hydrophobic amino acids. This remarkably different amino acid composition suggests that conformation of the C-termini of the two ZEB2 proteins would differ. Secondary structure analysis of the C-terminus of the wild-type and D1204Rfs*29 proteins using "Jpred consensus method for protein secondary structure prediction server" indicated a dramatically increased potential for alpha helix formation with strong hydrophobicity in the C-terminal peptide of ZEB2-D1204Rfs*29 [Cole et al., 2008]. This could affect the post-translational modifications of mutant ZEB2, including processing, phosphorylation, or glycosylation as well as protein stability, which could explain the Western blot findings. A different C-terminal frameshift mutation in ZEB2 has been reported in MWS where the c.3567-3568insCC frameshift mutation (causing a 2-bp insertion) produces a longer ZEB2 (p.M1190Pfs*50) than ZEB2-D1204Rfs*29; however, the characterization of the mutant ZEB2 has not been performed. The finding that nonsense mutations (1204X and 1210X) at the C-terminus of ZEB2 do not affect the protein stability suggests that these mutations may not cause typical MWS. To confirm these hypotheses, C-terminal analysis of the mutant ZEB2, case studies of MWS with C-terminus mutations, or single nucleotide polymorphism analyses of normal populations are necessary.

ACKNOWLEDGMENTS

We are grateful to the patients and their families for agreeing to participate in this study. Epidemiological survey was conducted by S.M. and K.K. This study was supported by the Takeda Science Foundation and a Health Labor Sciences Research Grant (to N.W.).

REFERENCES

Cacheux V, Dastot-Le Moal F, Kääriäinen H, Bondurand N, Rintala R, Boissier B, Wilson M, Mowat D, Goossens M. 2001. Loss-of-function mutations in *SIP1* Smad interacting protein 1 result in a syndromic Hirschsprung disease. Hum Mol Genet 10:1503–1510.

Cecconi M, Forzano F, Garavelli L, Pantaleoni C, Grasso M, Dagna Bricarelli F, Perroni L, Di Maria E, Faravelli F. 2008. Recurrence of Mowat–Wilson syndrome in siblings with a novel mutation in the *ZEB2* gene. Am J Med Genet Part A 146A:3095–3099.

Cole C, Barber JD, Barton GJ. 2008. The Jpred 3 secondary structure prediction server. Nucleic Acids Res 36:W197–W201.

Dastot-Le Moal F, Wilson M, Mowat D, Collot N, Niel F, Goossens M. 2007. *ZFHX1B* mutations in patients with Mowat–Wilson syndrome. Hum Mutat 28:313–321.

Evans E, Einfeld S, Mowat D, Taffe J, Tonge B, Wilson M. 2012. The behavioral phenotype of Mowat–Wilson syndrome. Am J Med Genet Part A 158A:358–366.

Garavelli L, Zollino M, Mainardi PC, Gurrieri F, Rivieri F, Soli F, Verri R, Albertini E, Favaron E, Zignani M, Orteschi D, Bianchi P, Faravelli F, Forzano F, Seri M, Wischmeijer A, Turchetti D, Pompilii E, Gnoli M, Cocchi G, Mazzanti L, Bergamaschi R, De Brasi D, Sperandeo MP, Mari F, Uliana V, Mostardini R, Cecconi M, Grasso M, Sassi S, Sebastio G, Renieri A, Silengo M, Bernasconi S, Wakamatsu N, Neri G. 2009. Mowat–Wilson syndrome: Facial phenotype changing with age: Study of 19 Italian patients and review of the literature. Am J Med Genet Part A 149A: 417–426.

Ishihara N, Yamada K, Yamada Y, Miura K, Kato J, Kuwabara N, Hara Y, Kobayashi Y, Hoshino K, Nomura Y, Mimaki M, Ohya K, Matsushima M, Nitta H, Tanaka K, Segawa M, Ohki T, Ezoe T, Kumagai T, Onuma A, Kuroda T, Yoneda M, Yamanaka T, Saeki M, Segawa M, Saji T, Nagaya M, Wakamatsu N. 2004. Clinical and molecular analysis of Mowat–Wilson syndrome associated with *ZFHX1B* mutations and deletions at 2q22-q24.1. J Med Genet 41:387–393.

Lurie IW, Supovitz KR, Rosenblum-Vos LS, Wulfsberg EA. 1994. Phenotypic variability of del(2)(q22-q23): Report of a case with a review of the literature. Genet Couns 5:11–14.

McGaughran J, Sinnott S, Dastot-Le Moal F, Wilson M, Mowat D, Sutton B, Goossens M. 2005. Recurrence of Mowat-Wilson syndrome in siblings with the same proven mutation. Am J Med Genet A 137A:302–304.

McKinsey GL, Lindtner S, Trzcinski B, Visel A, Pennacchio LA, Huylebroeck D, Higashi Y, Rubenstein JL. 2013. *Dlx1&2*-dependent expression of *Zfhx1b* (*Sip1*, *Zeb2*) regulates the fate switch between cortical and striatal interneurons. Neuron 77:83–98.

Mowat DR, Croaker GD, Cass DT, Kerr BA, Chaitow J, Adès LC, Chia NL, Wilson MJ. 1998. Hirschsprung disease, microcephaly, mental retardation, and characteristic facial features: Delineation of a new syndrome and identification of a locus at chromosome 2q22-q23. J Med Genet 35:617–623.

Mowat DR, Wilson MJ, Goossens M. 2003. Mowat–Wilson syndrome. J Med Genet 40:305–310.

Ohtsuka M, Oguni H, Ito Y, Nakayama T, Matsuo M, Osawa M, Saito K, Yamada Y, Wakamatsu N. 2008. Mowat–Wilson syndrome affecting 3 siblings. J Child Neurol 23:274–278.

Postigo AA, Depp JL, Taylor JJ, Kroll KL. 2003. Regulation of Smad signaling through a differential recruitment of coactivators and corepressors by ZEB proteins. EMBO J 22:2453–2462.

Sasongko TH, Sadewa AH, Gunadi Lee MJ, Koterazawa K, Nishio H. 2007. Nonsense mutations of the *ZFHX1B* gene in two Japanese girls with Mowat–Wilson syndrome. Kobe J Med Sci 53:157–162.

Seuntjens E, Nityanandam A, Miquelajauregui A, Debruyn J, Stryjewska A, Goebbels S, Nave KA, Huylebroeck D, Tarabykin V. 2009. Sip1 regulates sequential fate decisions by feedback signaling from postmitotic neurons to progenitors. Nat Neurosci 12:1373–1380.

Verschueren K, Remacle JE, Collart C, Kraft H, Baker BS, Tylzanowski P, Nelles L, Wuytens G, Su MT, Bodmer R, Smith JC, Huylebroeck D. 1999. SIP1, a novel zinc finger/homeodomain repressor, interacts with Smad proteins and binds to 5′-CACCT sequences in candidate target genes. J Biol Chem 274:20489–20498.

Verstappen G, van Grunsven LA, Michiels C, Van de Putte T, Souopgui J, Van Damme J, Bellefroid E, Vandekerckhove J, Huylebroeck D. 2008. Atypical Mowat–Wilson patient confirms the importance of the novel association between ZFHX1B/SIP1 and NuRD corepressor complex. Hum Mol Genet 17:1175–1183.

Wakamatsu N, Yamada Y, Yamada K, Ono T, Nomura N, Taniguchi H, Kitoh H, Mutoh N, Yamanaka T, Mushiake K, Kato K, Sonta S, Nagaya M. 2001. Mutations in *SIP1*, encoding Smad interacting protein-1, cause a form of Hirschsprung disease. Nat Genet 27:369–370.

Weng Q, Chen Y, Wang H, Xu X, Yang B, He Q, Shou W, Chen Y, Higashi Y, van den Berghe V, Seuntjens E, Kernie SG, Bukshpun P, Sherr EH, Huylebroeck D, Lu QR. 2012. Dual-mode modulation of Smad signaling by Smad-interacting protein Sip1 is required for myelination in the central nervous system. Neuron 73:713–728.

Yamada K, Yamada Y, Nomura N, Miura K, Wakako R, Hayakawa C, Matsumoto A, Kumagai T, Yoshimura I, Miyazaki S, Kato K, Sonta S,

Ono H, Yamanaka T, Nagaya M, Wakamatsu N. 2001. Nonsense and frameshift mutations in *ZFHX1B*, encoding Smad-interacting protein 1, cause a complex developmental disorder with a great variety of clinical features. Am J Hum Genet 69:1178–1185.

Yamada K, Takado Y, Kato YS, Yamada Y, Ishiguro H, Wakamatsu N. 2013. Characterization of the mutant β-subunit of β-hexosaminidase for dimer formation responsible for the adult form of Sandhoff disease with the motor neuron disease phenotype. J Biochem 153:111–119.

Zweier C, Albrecht B, Mitulla B, Behrens R, Beese M, Gillessen-Kaesbach G, Rott HD, Rauch A. 2002. "Mowat–Wilson" syndrome with and without Hirschsprung disease is a distinct, recognizable multiple congenital anomalies-mental retardation syndrome caused by mutations in the zinc finger homeobox 1B gene. Am J Med Genet 108:177–181.

Zweier C, Temple IK, Beemer F, Zackai E, Lerman-Sagie T, Weschke B, Anderson CE, Rauch A. 2003. Characterisation of deletions of the *ZFHX1B* region and genotype–phenotype analysis in Mowat–Wilson syndrome. J Med Genet 40:601–605.

Zweier C, Thiel CT, Dufke A, Crow YJ, Meinecke P, Suri M, Ala-Mello S, Beemer F, Bernasconi S, Bianchi P, Bier A, Devriendt K, Dimitrov B, Firth H, Gallagher RC, Garavelli L, Gillessen-Kaesbach G, Hudgins L, Kääriäinen H, Karstens S, Krantz I, Mannhardt A, Medne L, Mücke J, Kibaek M, Krogh LN, Peippo M, Rittinger O, Schulz S, Schelley SL, Temple IK, Dennis NR, Van der Knaap MS, Wheeler P, Yerushalmi B, Zenker M, Seidel H, Lachmeijer A, Prescott T, Kraus C, Lowry RB, Rauch A. 2005. Clinical and mutational spectrum of Mowat–Wilson syndrome. Eur J Med Genet 48:97–111.

RESEARCH ARTICLE

AMERICAN JOURNAL OF medical genetics PART A

Microarray and FISH-Based Genotype–Phenotype Analysis of 22 Japanese Patients With Wolf–Hirschhorn Syndrome

Kenji Shimizu,[1,2] Keiko Wakui,[1] Tomoki Kosho,[1]* Nobuhiko Okamoto,[3] Seiji Mizuno,[4] Kazuya Itomi,[5] Shigeto Hattori,[6] Kimio Nishio,[7] Osamu Samura,[8] Yoshiyuki Kobayashi,[9] Yuko Kako,[10] Takashi Arai,[11] Tsutomu Oh-ishi,[11] Hiroshi Kawame,[12] Yoko Narumi,[1] Hirofumi Ohashi,[2] and Yoshimitsu Fukushima[1]

[1]Department of Medical Genetics, Shinshu University School of Medicine, Matsumoto, Japan

[2]Division of Medical Genetics, Saitama Children's Medical Center, Saitama, Japan

[3]Department of Medical Genetics, Osaka Medical Center and Research Institute for Maternal and Child Health, Osaka, Japan

[4]Department of Pediatrics, Central Hospital, Aichi Human Service Center, Kasugai, Aichi, Japan

[5]Department of Pediatric Neurology, Aichi Children's Health and Medical Center, Obu, Aichi, Japan

[6]Department of Pediatrics, Gunma University Hospital, Maebashi, Japan

[7]Department of Neonatology, Seirei-Hamamatsu General Hospital, Hamamatsu, Shizuoka, Japan

[8]Department of Obstetrics and Gynecology, NHO Kure Medical Center and Chugoku Cancer Center, Kure, Japan

[9]Department of Pediatrics, Hiroshima University Hospital, Hiroshima, Japan

[10]Department of Pediatrics, Showa University School of Medicine, Tokyo, Japan

[11]Division of Clinical Laboratory, Saitama Children's Medical Center, Saitama, Japan

[12]Department of Genetic Counseling, Graduate School of Humanities and Science, Ochanomizu University, Tokyo, Japan

Manuscript Received: 27 April 2013; Manuscript Accepted: 30 September 2013

Wolf–Hirschhorn syndrome (WHS) is a contiguous gene deletion syndrome of the distal 4p chromosome, characterized by craniofacial features, growth impairment, intellectual disability, and seizures. Although genotype–phenotype correlation studies have previously been published, several important issues remain to be elucidated including seizure severity. We present detailed clinical and molecular-cytogenetic findings from a microarray and fluorescence in situ hybridization (FISH)-based genotype–phenotype analysis of 22 Japanese WHS patients, the first large non-Western series. 4p deletions were terminal in 20 patients and interstitial in two, with deletion sizes ranging from 2.06 to 29.42 Mb. The new Wolf–Hirschhorn syndrome critical region (WHSCR2) was deleted in all cases, and duplication of other chromosomal regions occurred in four. Complex mosaicism was identified in two cases: two different 4p terminal deletions; a simple 4p terminal deletion and an unbalanced *translocation with the same* 4p breakpoint. Seizures began in infancy in 33% (2/6) of cases with small (<6 Mb) deletions and in 86% (12/14) of cases with larger deletions (>6 Mb). Status epilepticus occurred in 17% (1/6) with small deletions and in 87% (13/15) with larger deletions. Renal hypoplasia or dysplasia and structural ocular anomalies were more prevalent in those with larger deletions. A new susceptible region for seizure occurrence is suggested between 0.76 and 1.3 Mb from 4pter,

How to Cite this Article:
Shimizu K, Wakui K, Kosho T, Okamoto N, Mizuno S, Itomi K, Hattori S, Nishio K, Samura O, Kobayashi Y, Kako Y, Arai T, Oishi T, Kawame H, Narumi Y, Ohashi H, Fukushima Y. 2014. Microarray and FISH-based genotype–phenotype analysis of 22 Japanese patients with Wolf–Hirschhorn syndrome.
Am J Med Genet Part A 164A:597–609.

Conflict of interest: none.
Grant sponsor: Japanese Ministry of Health, Labour and Welfare.
*Correspondence to:
Tomoki Kosho, M.D., Department of Medical Genetics, Shinshu University School of Medicine, 3-1-1 Asahi, Matsumoto 390-8621, Japan.
E-mail: ktomoki@shinshu-u.ac.jp
Article first published online in Wiley Online Library (wileyonlinelibrary.com): 19 December 2013
DOI 10.1002/ajmg.a.36308

encompassing *CTBP1* and *CPLX1*, and distal to the previously-supposed candidate gene *LETM1*. The usefulness of bromide therapy for seizures and additional clinical features including hypercholesterolemia are also described.

Key words: Wolf–Hirschhorn syndrome; 4p deletion; microarray analysis; fluorescence in situ hybridization (FISH); mosaicism; genotype–phenotype correlation; seizures

INTRODUCTION

Wolf–Hirschhorn syndrome (WHS, OMIM#194190), first described independently by Hirschhorn et al. [1965] and Wolf et al. [1965], is a contiguous gene deletion syndrome of the distal 4p chromosome characterized by a distinctive facial appearance, pre- and postnatal growth impairment, intellectual disability, and seizures [Battaglia et al., 2008]. In recent years, chromosomal microarray-based analysis has enabled us to identify WHS patients harboring well-defined variable-sized 4p deletions with or without additional duplications of other chromosomal regions as a result of unbalanced derivatives determined by concurrent metaphase fluorescence in situ hybridization (FISH) analysis [South et al., 2008c; Zollino et al., 2008].

Detailed genotype–phenotype correlation studies have also been performed using FISH analysis [Battaglia et al., 1999; Zollino et al., 2000] and chromosomal microarray analysis [Battaglia et al., 2008; Maas et al., 2008; South et al., 2008c; Zollino et al., 2008]. Clinical severity generally correlates with deletion sizes, although co-existing duplicated chromosomal regions, sequence variation of the gene(s) in the non-deleted 4p region, and other genetic backgrounds can all contribute to phenotypic variation [South et al., 2008c; Zollino et al., 2008]. Seizures represent a major clinical challenge in patients with WHS [Battaglia et al., 2009]. A review by Zollino et al. [2008] showed a high prevalence of seizures in patients with WHS regardless of the deletion sizes: 96% in those with <3.5 Mb deletions, 80% in those with 5–18 Mb deletions, and 90% in those with >22 Mb deletions. However, it remains unclear whether the severity of seizures in WHS patients might correlate with deletion sizes.

A WHS critical region, responsible for cardinal WHS features such as distinctive faces, growth/developmental delay, and seizures, was initially mapped to a 165-kb interval (WHSCR1) involving the entire *WHSC2* gene and the proximal part of *WHSC1* [Wright et al., 1997]. Additional reports of WHS patients with deleted regions distal to WHSCR1 suggested a new critical region (WHSCR2) involving the distal part of *WHSC1* and the entire *LETM1* gene, and these two genes have been considered the molecular hallmark of WHS [Zollino et al., 2003; Rodriguez et al., 2005]. Indeed, *WHSC1* is hypothesized as the gene that contributes to the main WHS phenotype of developmental delay and characteristic facial features [Nimura et al., 2009; Izumi et al., 2010]. *LETM1*, encoding a mitochondrial Ca^{2+}/H^{+} antiporter [Jiang et al., 2009], is thought to be the major candidate gene for seizures in patients with WHS [Rauch et al., 2001; South et al., 2007], while *FGFRL1*, located distal to WHSCR1/WHSCR2 and involved in bone cartilage formation during embryonic development, might be another candidate gene for craniofacial features of WHS [Catela et al., 2009; Engbers et al., 2009]. Other genes localized around these critical regions might also contribute to the various features of WHS.

Here, we present detailed clinical, microarray, and FISH-based molecular-cytogenetic findings of 22 Japanese patients with WHS, representing the first large series in a non-Western country.

MATERIALS AND METHODS

Patients

Twenty-two WHS patients from eight hospitals were included in this study between January 2010 and February 2012. The diagnosis of WHS was made from clinical characteristics as well as G-banded karyotyping with or without FISH analysis using a WHSCR or 4p subtelomeric probe. Written informed consent was obtained from all parents of the patients. Clinical information was collected by the clinical geneticists of each hospital and reviewed by one of them (K.S.). Ethical approval for this study was granted by the Institutional Review Board of Shinshu University School of Medicine, Matsumoto, Japan.

Chromosomal Microarray Analysis

Genomic DNA was isolated using standard protocols from the peripheral blood leukocytes of each patient. Chromosomal microarray analysis was performed through two whole genome oligonucleotide-based array platforms. NimbleGen CGX Array™ (Roche NimbleGen, Inc., Madison, WI) was used in the analyses of 21 patients, and includes 134,829 probes with an average resolution of 35 kb throughout the genome and 10 kb in clinically significant regions. Procedures for DNA labeling and microarray analysis were performed according to the manufacturer's instructions. The fluorescence signals on array slides were analyzed using a NimbleScan™ (Roche NimbleGen, Inc.), and presentation of array results was obtained by Genoglyphix® Software (Signature Genomics Laboratories, Spokane, WA). The Agilent Human Genome Microarray Kit 244A™ (Agilent Technologies, Santa Clara, CA) was used in the analysis of one patient, and includes 243,504 probes with a median probe space of 7.4 and 13.4 kb in intragenic and intergenic genomic sequences, respectively. Labeling and hybridization were performed according to the manufacturer's instructions, followed by scanning with an Agilent Microarray Scanner™ and data extraction with Feature Extraction Software™ (v9.5.3). The results were analyzed using Cytogenomics 2.0 Software™ (Agilent Technologies). Genomic coordinates of both array results were indicated according to NCBI build 36 (hg 18).

Metaphase FISH Analysis

To confirm cytogenetic rearrangements resulting in 4p deletion, FISH analysis using Bacterial Artificial Chromosome (BAC) probes was performed on metaphase chromosomes from peripheral blood leukocytes of all patients. We selected BAC probes around deleted regions of 4p and around other terminal duplicated segments in patients who were predicted to have unbalanced rearrangements

according to microarray results. Parental blood samples, where available, were also assayed with metaphase FISH to define whether chromosomal derivatives were de novo or inherited from parental balanced rearrangements. When a mosaic chromosomal abnormality was detected by G-banded karyotyping or suspected by chromosomal microarray results that showed a lower absolute $\log_2$ ratio than observed in patients with complete deletions or duplications, FISH analysis was performed on over 30 cells to detect a mosaic ratio.

RESULTS

Molecular-Cytogenetic Findings

Molecular-cytogenetic findings are summarized in Table I. G-banded chromosome analysis at the 400–550 band level, which was performed prior to this study, was abnormal in 18/22 (82%) patients: with terminal deletions of 4p in eight patients, interstitial deletions in three, additional materials of unknown origin attached to 4p in six, and mosaic chromosomes for a del(4)(p15.3p16.1) cell line (interstitial deletion) and a normal 46,XX cell line in Patient 15. G-banded chromosomes were normal in other patients who were found to have a deletion of 4p by FISH analysis using a 4p subtelomeric probe.

Chromosomal microarray analysis revealed 4p deletions to be terminal in 20 patients and interstitial in the other 2 patients. Deletion sizes ranged from 2.06 to 29.42 Mb, and all included WHSCR2 (Fig. 1). In patients with 4p terminal deletions, those $\leq$5.26 Mb were not detected by G-banded karyotyping. Only three patients (Patients 10, 11, and 12) shared the same breakpoints between 8.77 Mb (minimum) and 9.41 Mb (maximum) from the 4p terminus, corresponding to the loci of olfactory receptor (OR) gene clusters. Duplicated chromosomal regions accompanied by 4p deletion included 772 kb of terminal 10q in Patient 1, 45.6 Mb of terminal 4q in Patient 3, 6.9 Mb of terminal 8p in Patient 11, and 1.27 Mb of terminal 11q in Patient 20. In Patient 20, $\log_2$ values for probes spanning the duplicated 11q region were approximately 0.365 (theoretical $\log_2$ value of non-mosaic duplication, 0.58), which suggested that the duplication was mosaic (Fig. 2A).

FISH analysis using BAC probes designed according to microarray results confirmed a derivative chromosome 4 consisting of a duplicated 4q segment on the deleted 4p in Patient 3, and unbalanced translocations between 4p and 10q in Patient 1, and between 4p and 8p in Patient 11. In Patient 20, metaphases with an unbalanced translocation, der(4)t(4;11)(p15.31;q25), were found in 22/30 cells; and those with a simple terminal deletion, del(4)(p15.31), were found in 8/30 cells. The breakpoint of 4p was considered to be identical in both cell lines (21.0 Mb from 4pter; *Fig. 2B, C*). *In Patient* 15, metaphases with del(4)(p15.33) (11.9–12.1 Mb deletion) were found in 45/56 cells and those with del(4)(p16.3) (2.48–2.66 Mb deletion) were found in 11/56 cells (Fig. 3B, C), although only the larger deletion was demonstrated in microarray analysis (Fig. 3A). In nine patients whose parental samples were available, eight were found to have de novo deletions and the other (Patient 11) was found to have a maternal unbalanced translocation.

Clinical Findings and Correlation With Genotype

Clinical findings are summarized in Table II and major structural defects are listed according to deletion size in Table III. We categorized patients according to their deletion sizes into "small" with 4p terminal deletions less than 6 Mb (Patients 1–6), "intermediate" with deletions ranging from 6 to 15 Mb (Patients 7–17), and "large" with deletions over 15 Mb (Patients 18–22).

Neurological Features

Seizures began in 20/21 (95%) patients within the first three years of life (1 month to 2 years and 6 months old). Patient 10 was excluded because he was only 7 months old at the time of this study and might be expected to develop seizures in the future. Only Patient 13, aged 12 years with an 8.8 Mb interstitial deletion, had no seizures. The onset of seizures was late, occurring over 1 year of age, in 4/6 (67%) patients with small deletions (<6 Mb); and it was early, under 1 year of age, in 12/14 (86%) patients with larger deletions (>6 Mb). Status epilepticus occurred in 14/20 (70%) patients: 1/6 (17%) in those with small deletions and 13/14 (93%) in those with larger deletions. Seizures were intractable in six patients of ages ranging from 9 months to 6 years (median, 3 years and 7 months old), while seizures improved or disappeared in 14 patients of ages ranging from 1 year and 8 months to 18 years (median, 6 years and 2 months old). Potassium or sodium bromide was administered to four patients and the daily dose of bromide was 450 mg in Patient 7, 560 mg in Patient 8, 200 mg in patient 14, and 400 mg in Patient 18 at the time of this study. Seizures decreased in all of these. Patient 7 and Patient 8 showed a particularly obvious improvement after bromide therapy started at the ages of 1 year and 3 years, respectively. Neuroimaging demonstrated structural central nervous system defects in 9/18 (50%) patients, including periventricular leukomalacia, ventricular enlargement, hypoplasia of the corpus callosum, and cerebral or cerebellar atrophy.

A total of 19/22 (86%) patients showed severe developmental delay, while the other 3 patients showed a moderate delay. Independent walking was achieved in seven patients, including one with no seizures and five with no history of status epileptics.

Other Clinical Findings

Typical craniofacial features were present in all the patients except for Patient 1 with the smallest sized deletion (2.06 Mb; Fig. 4A) and Patient 13 with an interstitial deletion (1.37–10.22 Mb; Fig. 4H), both showing subtle features without the Greek warrior helmet appearance. The severity of short stature varied among patients regardless of the deletion sizes and the deleted regions. Eleven patients with various deletion sizes required tube feeding because of insufficient oral feeding associated with hypotonia, poorly coordinated swallowing, and/or gastroesophageal reflux. Gastrostomy was performed in two patients with the largest and the second largest deletions because of persistent insufficient oral feeding, failure to thrive regardless of tube feeding, recurrent respiratory distress, hypoglycemia, and/or carnitine deficiency.

Congenital heart defects were seen in 19/22 patients (86%). Three patients without heart defects had smaller deletions of 2.93, 5.49, and 7.51 Mb. The observed heart defects were common types,

TABLE I. Summary of Molecular-Cytogenetic Analysis of 22 WHS Patients

		Array-CGH analysis						
Patient no.	G-Banded chromosomes	Location and minimal deletion size of 4p		Distal breakpoint from 4pter[a]	Proximal breakpoint from 4pter	Other unbalanced region and minimal size	Final 4p rearrangement studied with a-CGH and FISH	Inheritance
1	46,XX	4p16.3	2.06 Mb	1–(63,075)	2,061,942–2,071,068	dup(10)(q26.3), 772 kb	Unbalanced translocation der(4) t(4;10)(p16.3;q26.3)	
2	46,XX	4p16.3	2.29 Mb	1–(41,413)	2,294,435–2,313,104		Isolated terminal	
3	add(4)(p16)	4p16.3	2.93 Mb	1–(63,075)	2,934,119–2,941,688	dup(4)(q31.22q35.2), 45.6 Mb	der(4)(4qter→q31.22:p16.3→qter)	
4	46,XX	4p16.3p16.2	3.45 Mb	1–(63,075)	3,453,423–3,475,088		Isolated terminal	
5	46,XX	4p16.3p16.1	5.26 Mb	1–(63,075)	5,259,705–5,286,063		Isolated terminal	
6	del(4)(p16.1)	4p16.3p16.1	5.49 Mb	1–(33,860)	5,488,869–5,517,610		Isolated terminal	De novo
7	del(4)(p16.1)	4p16.3p16.1	6.92 Mb	1–(33,860)	6,920,095–6,944,615		Isolated terminal	
8	del(4)(p16.1)	4p16.3p16.1	7.51 Mb	1–(63,075)	7,509,074–7,525,657		Isolated terminal	
9	del(4)(p15.3p16)	4p16.3p16.1	8.09 Mb	1–(63,075)	8,089,462–8,126,238		Isolated terminal	
10	add(4)(p15.3)	4p16.3p16.1	8.77 Mb	1–(63,075)	8,772,114–9,414,321		Isolated terminal	
11	add(4)(p15.2)	4p16.3p16.1	8.77 Mb	1–(33,860)	8,772,114–9,414,321	dup(8)(p23.3p23.1), 6.9 Mb	Unbalanced translocation der(4) t(4;8)(p16.1;p23.1)	Maternal
12	del(4)(p16.1)	4p16.3p16.1	8.77 Mb	1–(33,860)	8,772,114–9,414,321		Isolated terminal	De novo
13	add(4)(p15.3)	4p16.3p16.1	8.85 Mb	1,329,023–1,370,178	10,219,850–10,254,956		Isolated interstitial	
14	add(4)(p15.2)	4p16.3p15.33	11.11 Mb	1–(63,075)	11,105,238–11,129,635		Isolated terminal	De novo
15	46,XY,del(4)(p15.3p16.1)[26]/46,XY[4]	4p16.3p15.33	12.01 Mb	1–(33,860)	12,006,591–12,044,138		mos.del(4)(p15.33)/del(4)(p16.3)	
16	del(4)(p15.3)	4p16.3p15.33	12.33 Mb	1–(33,860)	12,331,994–12,371,059		Isolated terminal	De novo
17	del(4)(p15.32-p16.3)	4p16.3p15.33	13.63 Mb	813,367–841,095	14,467,735–14,498,501		Isolated interstitial	De novo
18	add(4)(p15.2)	4p16.3p15.32	15.70 Mb	1–(63,075)	15,700,625–15,737,006		Isolated terminal	
19	del(4)(p15.3)	4p16.3p15.31	18.62 Mb	1–(63,075)	18,616,970–18,655,860		Isolated terminal	De novo
20	del(4)(p15.2p16)	4p16.3p15.31	21.00 Mb	1–(63,075)	20,992,651–21,031,043	dup(11)(q25), 1.27 Mb	mos.der(4)t(4;11)(p15.31;q25)/del(4)(p15.31)	De novo
21	del(4)(p15.1)	4p16.3p15.1	28.35 Mb	1–(33,860)	28,348,051–28,384,613		Isolated terminal	De novo
22	del(4)(p15.1)	4p16.3p15.1	29.42 Mb	1–(63,075)	29,416,450–29,451,155		Isolated terminal	

Genomic locations of array results are according to NCBI build 36 (hg 18).
[a]Distal breakpoints of 41,413, 33,860, and 63,075 actually show terminal 4p deletions because the probes designed for the region are nonspecific to 4pter.

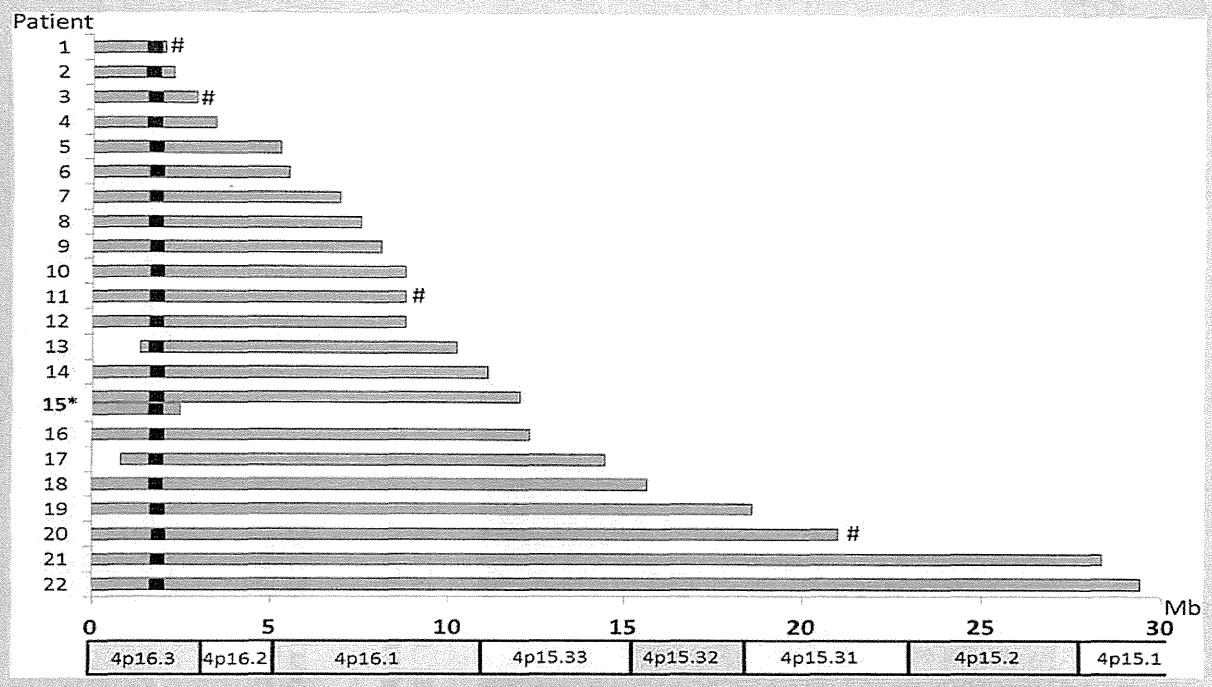

FIG. 1. Overview of 4p deletion sizes in each patient using chromosomal microarray analysis. Gray bars indicate deleted segments, black boxes indicate WHSCR2, and # denotes presence of other unbalanced regions. Patient 15 has a mosaicism with another minor cell line of a smaller-sized terminal deletion determined by metaphase FISH.

including atrial septal defects in 13 patients, pulmonary stenosis in six, and patent ductus arteriosus in five. The severity of the heart defects was not correlated with deletion sizes or deleted regions. No life-threatening complex heart defects were present in this series.

Structural urogenital anomalies were detected in a total of 47% (9/19) patients, including renal hypoplasia or dysplasia in six. The prevalence of patients with renal hypoplasia or dysplasia was 0/3 (0%) in the small deletion-type, 3/11 (27%) in the intermediate, and 3/5 (60%) in the large. Renal hypoplasia or dysplasia resulted in renal failure in five patients (83%).

Ophthalmologic abnormalities were detected in a total of 62% patients (13/21). Strabismus and nasolacrimal obstruction were found in patients with small or intermediate deletion-types, whereas structural ocular anomalies were found in patients with intermediate (2/11, 18%) and large (3/5, 60%) deletion-types. The prevalence of cleft lip/palate was 32% (7/22), that of skeletal abnormalities was 45% (9/20), and that of hearing impairment was 55% (12/22).

Other complications included hypercholesterolemia (>220 mg/dl) in a total of 36% (5/14) patients in whom serum cholesterol levels were examined, and the hypercholesterolemia was not familial in all the patients except one, whose parental information was not available. Multiple osteochondromatosis was observed in Patient 2 with a terminal 2.29 Mb deletion. The age of onset of osteochondromatosis was around 2 years. Radiological examination revealed a cartilage-capped bony growth arising from the area of the growth palate of the distal tibia and from the surface of the scapula. The patient underwent several surgical resections for progressive osteochondromatosis. Direct sequencing and multiplex ligation-dependent probe amplification analysis of *EXT1* and *EXT2*, the genes responsible for multiple osteochondromatosis (multiple exostosis type I (OMIM#133700) and type II (OMIM#133701), respectively) [Francannet et al., 2001], showed no pathogenic sequence variants.

DISCUSSION

In the current study, we performed microarray and FISH-based molecular-cytogenetic investigations of 22 Japanese patients with WHS, coupled with a detailed and comprehensive clinical evaluation. This resulted in identification of previously unreported complex chromosomal mosaicism and implication of several findings about the genotype–phenotype correlation including severity of seizures and structural anomalies.

Unbalanced translocations combined with a 4p deletion or other complicated rearrangement were identified in a total of four (18%) patients, which was lower than the recently reported frequency of 45% (15/33) by South et al. [2008c]. This discrepancy might be attributable to selection bias in both studies or the possible presence of a translocation with acrocentric p-arm in the current study, which could be detected through silver staining of the nucleolar organizing region (NOR), FISH using alpha satellite DNA probes, or parental FISH studies using a WHS-specific 4p16.3 probe [South et al., 2008c].

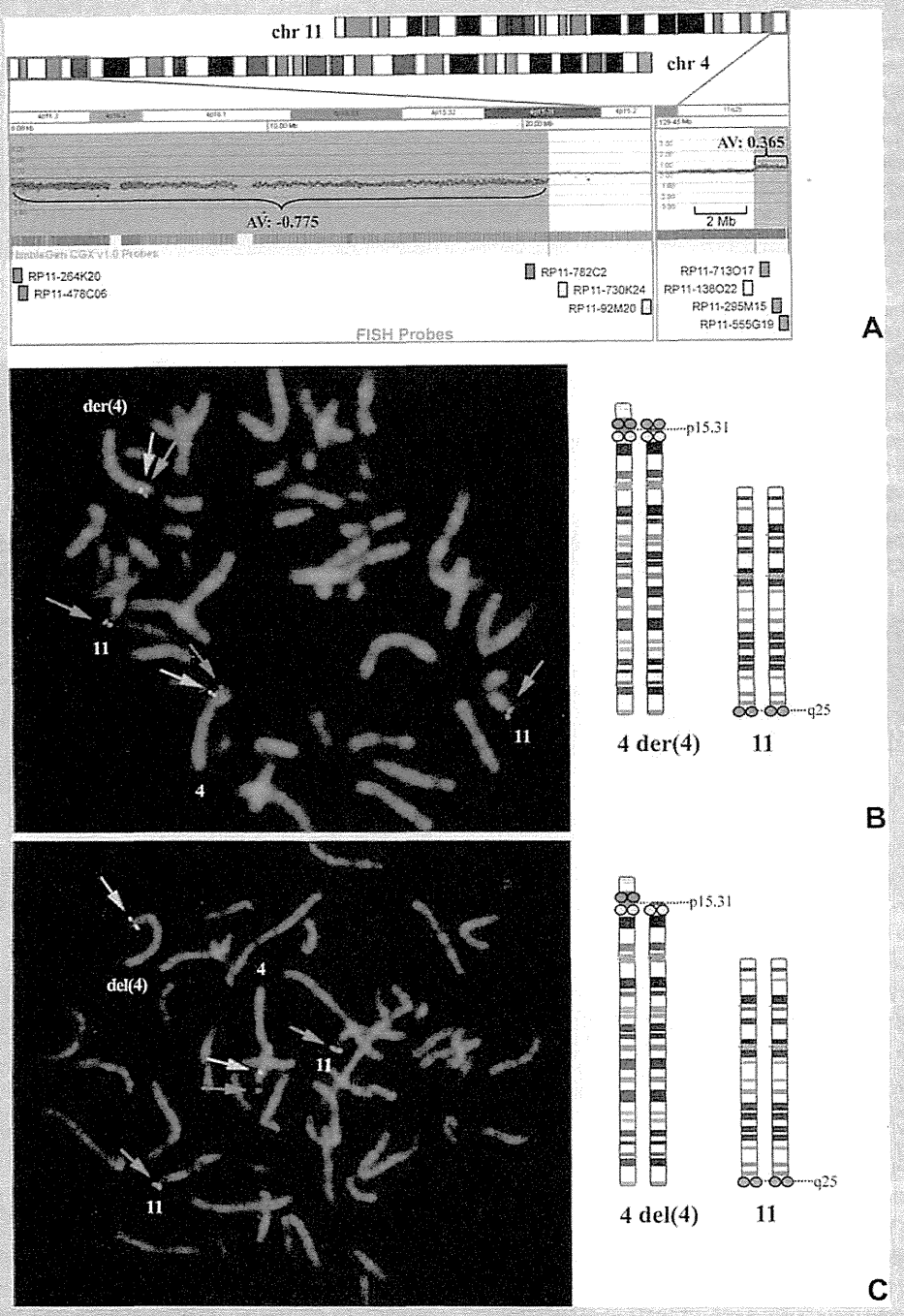

FIG. 2. Molecular-cytogenetic investigations of Patient 20. A: Upper panel shows microarray results. Whereas a 21.0-Mb copy number loss of 4pter with an average $\log_2$ value of −0.775 does not show a mosaicism, a 1.27-Mb copy number gain of 11qter with an average $\log_2$ value of 0.365 suggests a mosaicism. Lower panel shows BAC probes used in metaphase FISH. 4p probes deleted in both cell lines are shown in red, 11q probes duplicated in only the der(4)t(4;11) cell line are shown in green, and adjacent probes not deleted or duplicated in either cell line are shown in yellow at 4p or white at 11q. B: Metaphase FISH analysis showing the der(4)t(4;11) cell line. C: Metaphase FISH analysis showing the del(4) cell line. RP11-264K20 probe is shown in red, that for RP11-92M20 in yellow, and that for RP11-296M15 in green.

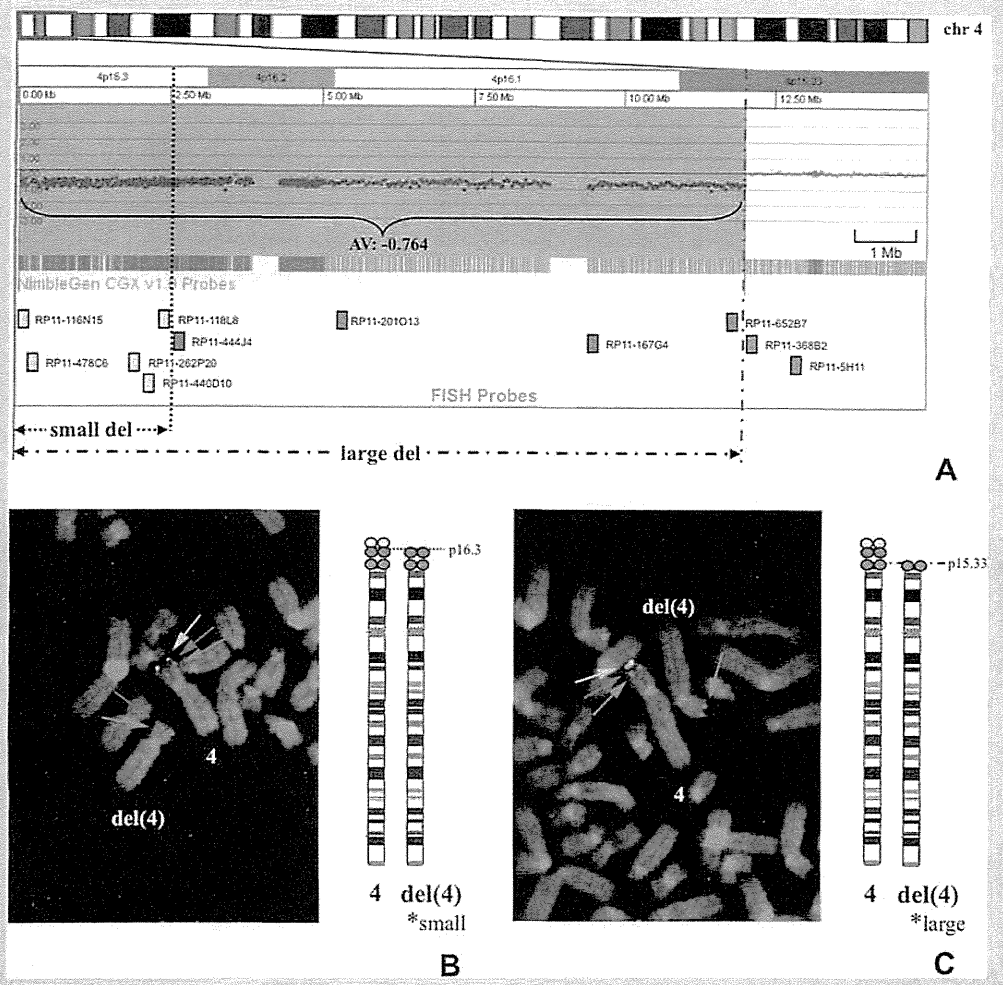

FIG. 3. Molecular-cytogenetic investigations of Patient 15. A: Upper panel shows microarray results. A 15-Mb copy number loss with an average $\log_2$ value of −0.764 does not suggest a mosaicism. Lower panel shows BAC probes used in metaphase FISH. Those deleted in both cell lines are shown in yellow, those deleted only in the cell line of the larger deletion are shown in red, and those not deleted in either cell line are shown in green. B: Metaphase FISH analysis showing the del(4)(p16.3) (2.48–2.66 Mb deletion) cell line. C: Metaphase FISH analysis showing the del(4)(p15.33) (11.9–12.1 Mb deletion) cell line. RP11-116N15 probe is shown in yellow that for RP11-118L8 in red, and that for RP11-652B7 in green.

Hitherto unreported patterns of complex mosaicism for two different structurally abnormal cell lines were identified in two of the patients in our current series using a combination of G-banding, microarray, and metaphase FISH analysis. Only a limited number of mosaicism cases have been previously reported of two cell lines both carrying 46 chromosomes and different structurally abnormal chromosomes, including del(8p)/inv dup del(8p) in several patients [Vermeesch et al., 2003; Pramparo et al., 2004; Hand et al., 2010]. Only one WHS patient was reported to carry two different structurally abnormal cell lines, del(4)(p16)/der(4)(qter-q31.3::pter–qter), which might have resulted from a meiotic crossing over event causing the der(4) cell line to be associated with a pericentric inversion and subsequent mitotic breakage [Syrrou et al., 2001]. A previous report showed expansion of a 4p terminal deletion between a mother and a son [Faravelli et al., 2007] and a subsequent report described this on 18q [South et al., 2008b]. Patient 15 might be another example of apparent instability of a terminal deletion, representing the expansion of a deletion within an individual rather than between generations.

Mosaicism of two different structurally abnormal cell lines, del(4)(p15.31)/der(4)t(4;11)(p15.31;q25), was indicated in Patient 20 by microarray through the lower $\log_2$ ratio of the duplicated 11q region. This supports the utility of microarray in that it can detect not only small copy number variation at a significantly higher resolution, but also detect mosaicism by incomplete $\log_2$ ratio compared with complete deletion or duplication [Ballif et al., 2006]. By contrast, mosaicism could not be detected in Patient 15 by microarray, perhaps because of the different levels of mosai-